Radiation Physics and Chemistry 207 (2023) 110878

Contents lists available at ScienceDirect

Radiation Physics and Chemistry

journal homepage: www.elsevier.com/locate/radphyschem

A dosimetric comparison between ICRP and ORNL phantoms from exposure to ^{137}Cs contaminated soil

Milena Živković [a], Mehrdad Shahmohammadi Beni [b,c], Peter K.N. Yu [b], Hiroshi Watabe [c], Dragana Krstić [a], Dragoslav Nikezić [a,d,*]

[a] University of Kragujevac, Faculty of Science, R. Domanovica 12, 34000, Kragujevac, Serbia
[b] Department of Physics, City University of Hong Kong, Tat, Chee Avenue, Kowloon Tong, Hong Kong, China
[c] Division of Radiation Protection and Safety Control, Cyclotron and Radioisotope Center, Tohoku University, 6-3 Aoba, Aramaki, Aoba-ku, Sendai, Miyagi, 980-8578, Japan
[d] The State University of Novi Pazar, Vuka Karadzica 9, 36300, Novi Pazar, Serbia

ARTICLE INFO

Handling Editor: Dr. Chris Chantler

Keywords:
^{137}Cs
ICRP
ORNL
MCNP
Open-source program

ABSTRACT

The ^{137}Cs soil contamination has detrimental effects on human health. The penetration and distribution of ^{137}Cs radionuclides at different soil depths were investigated. Two sampling campaigns in 2001 and 2018 were performed to determine the ^{137}Cs activity in soil at 11 locations around the city of Kragujevac in central Serbia. The ICRP and ORNL humanoid phantom models were used to determine equivalent and effective doses from the experimentally measured data, and conversion coefficients were obtained from Monte Carlo computations. The results show a general decrease in ^{137}Cs concentration in samples that were taken in 2018. However, variation of ^{137}Cs concentration was observed at different locations that did not match the expected reduction of ^{137}Cs concentration based on its half-life.

Considering the computational results, no significant difference between the estimated equivalent dose rate per unit activity of ^{137}Cs (conversion coefficients) between ICRP and ORNL phantoms was observed. In addition, two open-source computer programs for PC and Android devices were developed for users to determine the equivalent and effective doses for their specific cases; this gives the users an easy-to-use interface and portable tools to determine dosimetric quantities. The obtained results and the developed tools would be useful for future investigations related to soil contamination by ^{137}Cs radionuclides that require extensive future studies.

1. Introduction

^{137}Cs is a fission product that emits 661.6 keV photons with a yield of 85.1% and the exposure to the emitted ionizing radiation from ^{137}Cs was found to have detrimental effects on human health. The ^{137}Cs originated from atmospheric nuclear tests until late 1960 and from the Chernobyl accident, which occurred in 1986 (UNSCEAR, 2008). Compared to the Chernobyl accident, the Fukushima accident in 2011 (Koo et al., 2014) did not contribute to significant contamination of Europe (Steinhauser et al., 2014; Wai et al., 2020). Through dry and wet deposition, ^{137}Cs was deposited on the soil surface, and then by diffusion, convection, and other processes it penetrated into the deeper layers of the soil reaching plants' root, and then through the food chain into the human body. Based on our latest study (Zivkovic et al., 2022), ^{137}Cs penetrated the subsurface layer of the soil, to a depth of more than 15 cm. Previous studies (Krstić et al., 2004; Krstić and Nikezić, 2006; Zivkovic et al., 2022) investigated the vertical distribution of ^{137}Cs in soil both experimentally and theoretically. The experiments referred to two sampling periods of 2001 and 2018 that corresponded to about half of its half-life in 2001 and slightly more than one elapsed half-life in 2018, with respect to the Chernobyl accident from 1986.

The International Commission on Radiological Protection (ICRP) adopted the voxel models for their computational phantoms to represent the Reference Computing Phantoms of the Human Body Adult Male (RCP-AM) and Female (RCP-AF) (ICRP110, 2009). Based on ICRP publication 110 (ICRP110, 2009), phantoms of both sexes were created based on CT data, which were obtained from real human bodies. The geometry and sizes of organs and tissues, together with their compositions and densities were shown in ICRP publication 110 (ICRP110, 2009). Within the European Radiation Dosimetry Group (EURADOS),

* Corresponding author. The State University of Novi Pazar, Vuka Karadzica 9, 36300, Novi Pazar, Serbia.
E-mail address: nikezic@kg.ac.rs (D. Nikezić).

https://doi.org/10.1016/j.radphyschem.2023.110878
Received 6 December 2022; Received in revised form 23 February 2023; Accepted 26 February 2023
Available online 28 February 2023

inter-comparison between different simulation software was performed using RCP-AM and RCP-AF voxel phantoms under different irradiation scenarios (Zankl et al., 2021; Eakins et al., 2021; Gómez-Ros et al., 2021; Huet et al., 2022). One of the tasks was related to the phantom "standing" on the soil which was contaminated with ^{241}Am (Eakins et al., 2021). The irradiation geometry used in the present paper was similar to that used in the abovementioned task given by EURADOS group, however, the soil was considered to be inhomogeneously contaminated with ^{137}Cs radionuclides.

In the present work, the conversion coefficients (i.e., the equivalent and effective dose rates per unit activity of ^{137}Cs in soil, as the source of external ionizing radiation) were calculated for individual organs and tissues in the human body for ICRP voxel and ORNL phantoms (Cristy and Eckerman, 1987; Krstic and Nikezic, 2007). The Monte Carlo N-Particle (MCNP) code version 6.2 (Werner et al., MCNP User's Manual, Code Version 6.2., 2017) was employed to perform the radiation transport computations and to calculate the doses in all major organs of the human body, as well as in the remaining organs exposed to ^{137}Cs in the soil. From the obtained results, the equivalent and effective dose rates from exposure to ^{137}Cs contaminated soil were determined.

In addition, an open-source graphical user interface (GUI) was developed. The users have the ability to determine the equivalent doses for different organs and effective doses for their experimentally measured ^{137}Cs activity in soil by choosing four different humanoid phantoms, namely, male/female ICRP110 and male/female ORNL phantoms. The present results and the developed program would be useful for the field of radiation dosimetry for ^{137}Cs inhomogeneously contaminated soils.

2. Materials and methods

2.1. Modelled ICRP phantom

The auxiliary files named AM.DAT and AF.DAT in DAT format were provided in ICRP110. In these DAT files, a string of numbers represented the voxels with the corresponding ID number (i.e., material ID) which was used to fill a particular voxel. Each material number in the AM.DAT and AF.DAT files corresponded to a specific chemical composition and density. A total of 141 organs/tissues were presented in this model (including air within and out of the human body) and could be found in Tables A1 and A.2 in Annex A of ICRP Publication 110 (ICRP, 2009).

The orientation of the three-dimensional array of voxels describing the computational phantom was given by the columns corresponding to the *x* coordinates (note that the column numbers increase from right to left of the phantom body). The rows corresponded to the *y* coordinates (note that the row numbers increased from front to back of the phantom body). The slices corresponded to the *z* coordinates (slice numbers increase from the toes up to the vertex of the phantom body) (ICRP110). The AM.DAT file defined a grid of 7,161,276 voxels, 254 in the *x*-axis direction, 127 in the *y*-axis direction, and 222 in the *z*-axis direction, in a parallelepiped measuring 54.2798 × 27.1399 × 177.6 cm^3 and the size of 1 voxel was 0.2137 × 0.2137 × 0.8 cm^3. Each voxel which belonged to a certain organ or tissue was filled with the appropriate material with a defined ID number and density. Each of the materials had a certain chemical composition and density, so they were defined at 1 or 100% in terms of chemical composition. All materials were defined in the input file in the "map" medium section and the total number of defined media was 53. The AF.DAT file referred to a female RCP, containing 14,255,124 voxels, 299 in the *x*-axis direction, 137 in the *y*-axis direction, and 348 in the *z*-axis direction, with a voxel size of 0.1775 × 0.1775 × 0.484 cm^3. The corresponding parallelepiped for the female phantom had dimensions: 53.0725 × 24.3175 × 168.432 cm^3.

2.2. Modelled ORNL phantom

Oak Ridge National Laboratory (ORNL) proposed analytical equations to model the human body and these data were used to generate mathematical phantoms of the human body for the MCNP5 package (X-5 Monte Carlo Team, 2003). Previously developed ORNL phantoms (Krstic and Nikezic, 2007; Goorley, 2007) have been used to determine the conversion coefficients for different organs for exposure to ^{137}Cs contaminated soil at different depths. Considering the wide use of the ORNL phantoms in various studies (Han et al., 2006; Krstic et al., 2014; Lamart et al., 2011; Miri et al., 2012; Xu, 2014), it would be pertinent to report these conversion coefficients and compare them with ICRP voxel phantom data. The comparison between the ORNL and ICRP voxel phantoms was performed for ^{137}Cs contamination at the same soil depth, and the results were summarized in the present paper.

Table 1
Conversion coefficients (equivalent dose rate per unit activity of ^{137}Cs in soil) for male and female ICRP phantoms, in different organs as a function on depth in soil. AM male phantom, and AF female phantom.

Equivalent dose rate per unit activity of ^{137}Cs in soil (fSv.s^{-1})/(Bq.kg^{-1}))						
Organ	Depth (cm) →	0–5	5–10	10–15	15–20	0–20
	Phantom					
RBM	AM	6.6	2.6	1.0	0.4	10.9
	AF	7.2	2.8	1.1	0.5	11.5
Colon	AM	7.9	3.1	1.2	0.5	12.9
	AF	8.3	3.1	1.2	0.5	13.2
Lung	AM	6.4	2.5	1.0	0.4	10.5
	AF	7.3	2.9	1.2	0.5	11.9
Stomach	AM	6.8	2.7	1.1	0.5	10.7
	AF	7.8	3.0	1.1	0.5	12.6
Breast	AM	8.5	3.6	1.5	0.6	12.1
	AF	8.6	3.5	1.5	0.6	13.9
Remainder	AM	7.1	2.8	1.2	0.5	11.4
Tissues	AF	7.7	3.0	1.2	0.5	12.3
Gonads	AM	12.4	4.5	1.8	0.8	18.0
	AF	9.3	3.4	1.3	0.6	13.9
Bladder	AM	8.1	3	1.2	0.5	12.5
	AF	9.8	3.6	1.3	0.6	14.5
Esophagus	AM	5.3	2.2	0.8	0.3	8.3
	AF	6.5	2.5	1.0	0.4	10.1
Liver	AM	6.7	2.7	1.1	0.4	11.0
	AF	7.5	2.9	1.2	0.5	11.9
Thyroid	AM	5.7	2.2	0.8	0.4	8.4
	AF	6.4	2.5	1.1	0.4	10.6
Endosteum	AM	9.5	3.4	1.4	0.6	15.0
	AF	9.8	3.5	1.4	0.6	15.3
Brain	AM	5.6	2.4	1.0	0.4	9.4
	AF	6.2	2.6	1.1	0.4	10.4
Salivary glands	AM	6.7	2.8	1.2	0.5	10.8
	AF	6.9	3.0	1.2	0.5	11.5
Skin	AM	12.3	4.5	1.9	0.8	19.4
	AF	12.7	4.6	1.9	0.8	20.1

2.3. Soil sampling and ^{137}Cs activity measurements

Soil sampling was conducted at locations near the city of Kragujevac in central Serbia in 2018. The sampling locations were chosen to be as close as possible to the same places as in first sampling campaign in 2001. The experimental procedure and radioactivity measurement protocols were described in the previous work (Zivkovic et al., 2022). Activity concentrations of ^{137}Cs were measured in the soil layers from 0 to 5 cm, 5–10 cm, 10–15 cm, 15–20 cm, and 0–20 cm, respectively. These were different from those in the previous sampling/measurements campaign where the layers were 2 cm thick. Measurements were performed with a High Purity Germanium (HPGe) spectrometry (GEM30-70, ORTEC) system with 30% of relative efficiency and an energy resolution of 1.85 keV FWHM for ^{60}Co at 1.33 MeV. Detector calibration was performed with the calibration source provided by Czech Metrological Institute. The calibration source was contained in a Marinelli beaker with a volume of 450 mL, which consisted of a mixture of the following radioisotopes: ^{241}Am, ^{109}Cd, ^{139}Ce, ^{57}Co, ^{60}Co, ^{137}Cs,

^{113}Sn, ^{85}Sr, ^{88}Y, ^{203}Hg and ^{152}Eu). The total activity of the source was 40.01 kBq. Quality assurance was verified through several extensive tests which were organized by IAEA in years 2019 and 2021, and good agreement was found in comparison to the targeted values provided by IAEA (2004).

2.4. Monte Carlo computations with MCNP6.2

An input file for MCNP6.2 was created for the male and female ICRP and ORNL humanoid phantoms. The supplementary data files AM.DAT and AF.DAT that were provided by ICRP110 were used as a basis to create voxel phantoms in the voxelization process. For this purpose, Intel FORTRAN was used to calculate the coordinates of all voxel's vertex, and the repetition property of voxel elements in the MCNP code was applied. Each organ of the phantom contained a certain number of voxels filled with the appropriate material; and the organs were defined in a rectangular prism with minimum/maximum columns, rows, and slices occupied by the organ/tissue. The input file first defined the cell map, then the surface map, which was followed by the definition of the source and finally the tallies were defined (i.e., the desired user output). To calculate the deposited energy in the organs and tissues of the human body, F6 tally was applied, which by default represented the deposited energy in units of MeV/g per *primary source particle*. To determine the dependence of conversion coefficients on the depth, one main large cylinder of soil was divided into 4 smaller cylinders each with a thickness of 5 cm, and thus a total thickness of 20 cm. This further meant that 5 input files were created for each phantom (both ICRP and ORNL). In this way, totally 20 input files were made, where the irradiation source was a soil cylinder with a height of 5 cm at various depths. The modelled ICRP and ORNL male and female phantoms are shown in Fig. 1. The phantoms were placed at the center of the soil surface, which was considered as the radiation source emitting 661.6 keV photons. The soil sample was modelled as a cylinder with a radius of 300 cm and a height of 20 cm. Photons emitted from the points deep in the soil and furthered than 300 cm travelled longer path lengths in the soil and had a larger probability for absorption. In addition, photons emitted further than 3 m from a phantom have small probabilities to hit the target. Numerical experiments showed that 300 cm was good choice, because contribution from photons emitted further than 3 m was too small, and they were neglected in this work. The soil density was 2.3 g/cm^3 and the data on soil composition were taken from Eakins et al. (2021).

The phantom was surrounded by ambient air that corresponded to the realistic situation. A similar setup was used for the ORNL phantom irradiation so that the obtained results could be compared.

Separate simulations were performed for male and female voxel phantoms for each soil layer. It needs to be noted that the Monte Carlo (MC) simulations of voxel phantoms are very complex; therefore, the input files would be very large and computationally expensive. Therefore, employing cluster computers for such computations would be highly recommended. In the present work, all computations (for a total of eight input files for different cases) were performed on the cloud cluster InSPECT (International Secure Platform for Export-Controlled Computing Tools, located in US) (https://www.ornl.gov/onramp/computing-resources). Each run utilized 16 cores, while the average simulation time was approximately 400 and 2000 min for ORNL and ICRP phantoms, respectively.

2.5. Effective and equivalent doses

The equivalent dose H_T in an organ or tissue T was calculated from the *mean* absorbed dose in that tissue ($D_{T,R}$) as: $H_T = \sum_R w_R D_{T,R}$, where w_R was the radiation weighting factor for radiation R, and the absorbed dose was calculated as the energy deposited in the organ divided by the organ mass. The unit for absorbed dose is Gray, Gy = J kg^{-1}.

To estimate the effective dose, which is weighting average equivalent dose in organs of human body, tissue weighting factors are needed, and they were adopted from ICRP103 (ICRP103, 2007).

The ICRP Publication 103 (ICRP103, 2007) considered 15 major organs including red bone marrow (RBM), colon, lungs, stomach, gonads, bladder, esophagus, liver, thyroid, endosteum (bone surface), brain, salivary glands, skin, and remainder tissues. The main problems that arose were estimation of absorbed dose in bone, especially for the red bone marrow and the endosteum (former name: bone surface). For dosimetry calculations in the red bone marrow and endosteum, the mass-weighted average of doses described in ICRP 116 was applied (ICRP116, 2010). The absorbed dose to active marrow D_{skel} (*AM*) and the absorbed dose to endosteum D_{skel} (*TM50*) are determined according to the mentioned methods:

$$D_{skel}(AM) = \frac{\sum m(AM,x)}{m(AM)} D(SP,x) \quad (1)$$

$$D_{skel}(TM50) = \frac{\sum m(TM50,x)}{m(TM50)} D(SP,x) + \frac{\sum m(TM50,x)}{m(TM50)} D(MM,x) \quad (2)$$

where $m(AM,x)$ and $m(TM50,x)$ are masses of active marrow and endosteum in skeletal at site x, respectively, as given in Table 3.2 in the ICRP publication (ICRP116, 2010), $D(SP,x)$ and $D(MM,x)$ are the absorbed doses to spongiosa and to medullary marrow in bone at site x, respectively; $m(AM)$ and $m(TM50)$ are the masses of active marrow and mass of endosteum summed across the entire skeleton, respectively.

The remainder tissues are made up of 13 organs, which are adrenal glands, extra thoracic region, gallbladder, heart, kidneys, lymph glands, oral mucosa, prostate (male), small intestine, spleen, pancreas, thymus and uterus/cervix (for female phantom). All remainder organs are treated as one organ using an arithmetic mean with a tissue weighting factor of 0.12. It needs to be noted that breast was omitted for the male ORNL phantom. In addition, the salivary glands were omitted for both

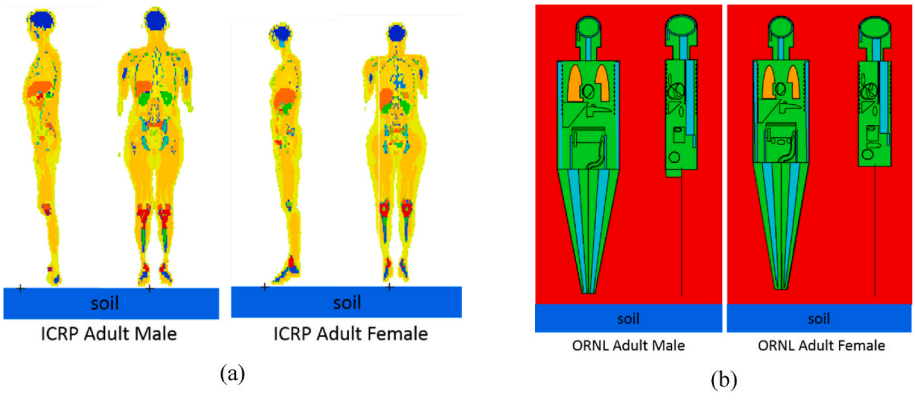

Fig. 1. Modelled male and female (a) ICRP and (b) ORNL phantoms placed on the surface of the soil.

male and female ORNL phantoms. Lastly, the brain was integrated with remainder of organs for the modelled ORNL phantoms. It needs to be noted that brain and salivary glands were not included in main organs when ORNL phantom was created.

The effective dose was calculated by averaging the equivalent doses of male and female organs, using the following formula:

$$E = \sum_i w_T \left(\frac{H_{T,m} + H_{T,f}}{2} \right) \quad (3)$$

where $H_{T,m}$ and $H_{T,f}$ were the equivalent organ doses for the male and female phantoms, respectively.

The results from the tally F6 were obtained from the generated output files using the MCNP package. Since the results from the F6 tally were deposited energy in units of MeV/g *per photon*, it was necessary to convert them to Gy per photon by multiplying with a factor of 1.602×10^{-10}. Since the radiation weighting factor for gamma photons is 1, the obtained numerical values would be equal to those of equivalent doses, in Sv per photon. In addition, multiplying the previous results with the number of photons emitted by the cylindrical source per second (assuming that volumetric activity was 1 Bq•m^{-3}) would lead to conversion to the unit (fSv/s)/(Bq.kg^{-1}).

2.6. The GUI dosimetric program and android version

The raw data that were obtained from MC computations were used to calculate equivalent and effective doses for different phantoms. A dedicated open-source GUI program was developed using the C++ programming language for determination of equivalent doses for different organs using the obtained conversion coefficients. The program takes the phantom type, organ, ^{137}Cs concentration activity, and the depth in soil to compute and report the conversion coefficient value for the chosen organ, equivalent, and effective doses. The program GUI was built using QT5 libraries (https://www.qt.io/) in a portable fashion where users are not required to install the program. The program consisted of ~1100 lines of code compiled on both GNU/Linux and Microsoft Windows operating systems. The GUI of the developed program is shown in Fig. 2.

In addition to the developed PC version of the dosimetric program that can determine conversion coefficients, equivalent and effective dose values for four different phantoms, we have developed a portable open-source android version of our program. The android version of the program provides users with much higher portability as the users can input the ^{137}Cs activity concentrations measured onsite and get the results rather instantly. The screenshot from the developed android app is shown in Fig. 3. The android app was developed using Android Studio (https://developer.android.com/studio) in Java programming language. All executables and full source code of the developed program can be downloaded from:

https://figshare.com/articles/software/A_dosimetric_comparison_between_ICRP_and_ORNL_phantoms_from_exposure_to_137Cs_contaminated_soil/21640661.

3. Results and discussion

3.1. Conversion coefficients for different organs

The results for male and female ICRP and ORNL phantom organs and tissues for different soil depths are shown in Tables 1 and 2, respectively. The first column of Tables 1 and 2 shows the organs of phantoms. The second column shows the phantom gender that would be either adult male (AM) or adult female (AF) phantoms. The other columns show the conversion coefficients of the equivalent dose rate per unit specific activity for the organs of the phantom of both sexes in (fSvs^{-1})/(Bq.kg^{-1}) with the soil depth as parameter. The highest conversion coefficient was obtained for skin in the range from 0.8 to 12.7 (fSvs^{-1})/(Bq.kg^{-1}), which agrees with the result of our previous work (Krstić and Nikezić, 2006). A similar trend was obtained for the ORNL phantoms, and the range of conversion coefficient for skin was found to be from 0.7 to 15.5 (fSvs^{-1})/(Bq.kg^{-1}). This was mainly due to the higher absorbed doses in

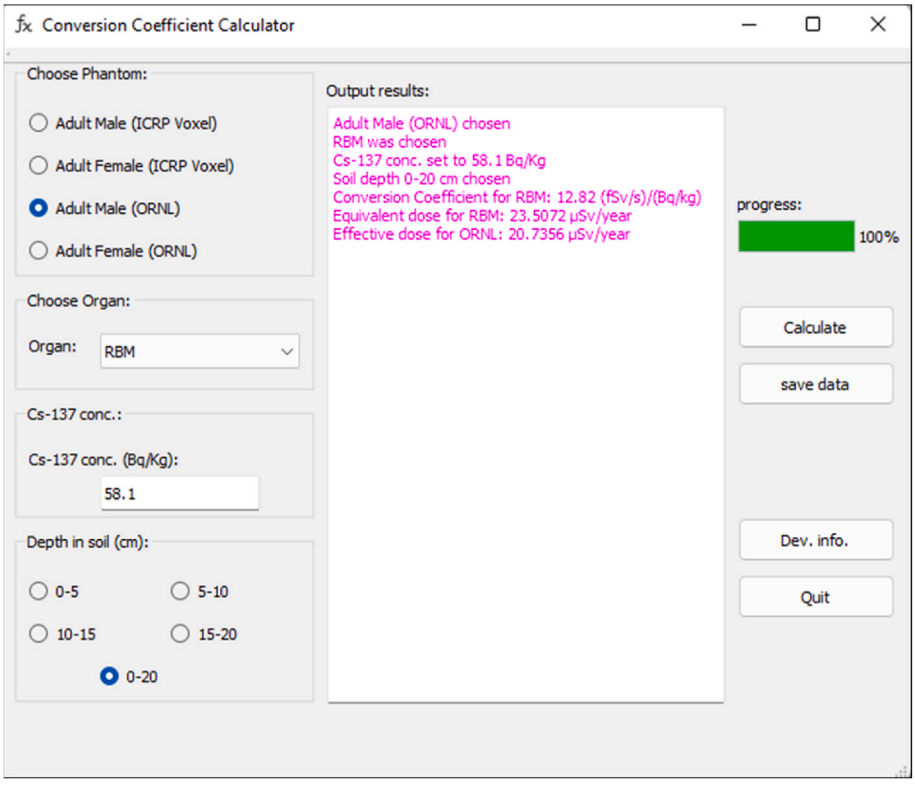

Fig. 2. Snapshot of dosimetric program GUI in action.

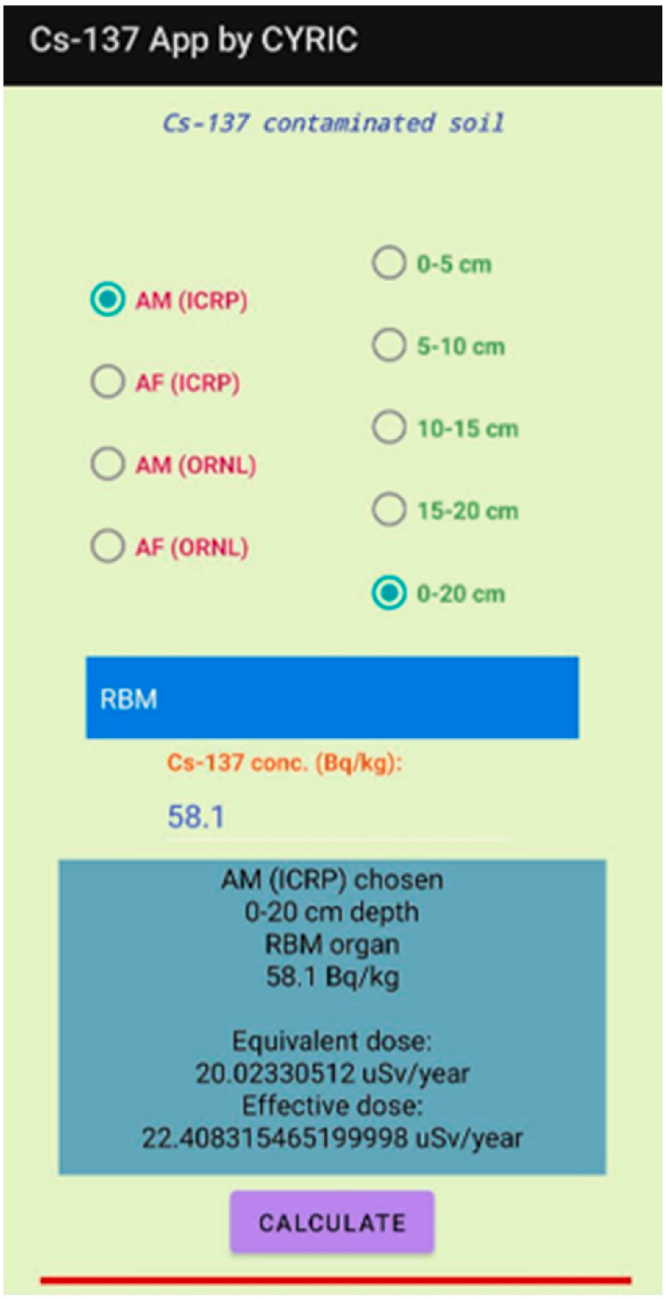

Fig. 3. Snapshot of android version of the dosimetric program in action.

the organs that were distributed in the body such as skin. In addition, the urinary bladder, colon, and gonads were found to have the highest absorbed dose, mainly since those organs were closest to the source of radiation. In contrast, the lowest absorbed dose was found to be in esophagus and thyroid gland; this was mainly due to the locations of these organs that were farthest away from the source of radiation. Table 3 shows differences (in %) between conversion coefficients of organs and tissues for both phantoms. The largest difference is for small organs, namely, thyroid and gonads. These two organs were defined in different ways in ORNL and ICRP approaches, which could be the reason for such a large discrepancy. The difference is also significant for red bone marrow because different methods were used for dose estimation. In some organs, the ICRP phantom produces smaller doses (RBM and endosteum), while it is opposite in other organs (remainder tissues, gonads and thyroid).

Table 2
Conversion coefficients (equivalent dose rate per unit activity of ^{137}Cs in soil) for male and female ORNL phantoms, in different organs as a function on depth in soil. AM male phantom, and AF female phantom.

Equivalent dose rate per unit activity of ^{137}Cs in soil (fSv.s^{-1})/(Bq.kg^{-1}))						
Organ	Depth (cm) →	0–5	5–10	10–15	15–20	0–20
	Phantom					
RBM	AM	7.8	3.2	1.3	0.6	12.8
	AF	9.0	3.6	1.5	0.6	14.7
Colon	AM	7.7	2.8	1.1	0.4	12.1
	AF	8.4	3.0	1.2	0.5	13.2
Lung	AM	6.9	2.8	1.1	0.5	11.2
	AF	7.3	2.9	1.2	0.5	11.8
Stomach	AM	7.5	2.9	1.2	0.5	12.0
	AF	7.6	2.9	1.1	0.5	12.0
Breast	AM	–	–	–	–	–
	AF	9.3	3.9	1.7	0.7	15.4
Remainder	AM	6.5	2.5	1.0	0.4	10.3
Tissues	AF	7.1	2.7	1.1	0.4	11.3
Gonads	AM	9.5	3.5	1.4	0.6	15.1
	AF	8.3	3.0	1.2	0.5	13.2
Bladder	AM	8.5	3.1	1.2	0.5	13.3
	AF	9.3	3.4	1.4	0.6	14.7
Esophagus	AM	5.5	2.2	0.8	0.1	8.8
	AF	6.1	2.3	0.9	0.4	9.7
Liver	AM	7.0	2.7	1.1	0.4	11.2
	AF	7.5	2.9	1.2	0.5	12.0
Thyroid	AM	2.0	0.8	0.3	0.1	3.3
	AF	4.1	1.6	0.7	0.3	6.6
Endosteum	AM	9.8	3.7	1.5	0.6	15.6
	AF	9.9	3.8	1.6	0.7	15.8
Brain	AM	–	–	–	–	–
	AF	–	–	–	–	–
Salivary glands	AM	–	–	–	–	–
	AF	–	–	–	–	–
Skin	AM	11.4	4.2	1.7	0.7	18.1
	AF	15.5	5.5	2.3	1.0	24.3

3.2. ^{137}Cs measurements and calculations of equivalent and effective dose

The conversion coefficients given in Tables 1 and 2 were used to calculate the effective doses from ^{137}Cs upon knowing its activity concentrations at individual locations from field measurements (Zivkovic et al., 2022). Table shows the activity concentrations of ^{137}Cs measured in two sampling campaigns, at 2001 and 2018 in 11 locations (Krstić and Nikezić, 2006). All details about sampling procedure, preparation of soil samples, gamma spectrometry measurements, as well as depth profiles and data for ^{137}Cs at all locations were described in Zivkovic et al. (2022) In general, the activities obtained from samples taken from 2018 were lower than those from 2001, except for the sample collected at location 6. It was expected that the activities would be reduced by about 32.5%, but such reduction was not satisfied in any case. There were large discrepancies between the expected and measured values. As mentioned, the activities at locations 6 and 11 were found to be much higher in 2018 when compared to 2001. There could be several explanations, including: (1) the sampling sites were not exactly the same, since different individuals performed the sampling in two different campaigns, (2) the soil at the sampling site might have been disturbed so that the vertical profile of ^{137}Cs was not preserved (3) there are other unknown processes which influence the concentrations of ^{137}Cs in soil.

The equivalent doses were calculated using the present computer program for 6 different organs using the ^{137}Cs activity concentration at location 1 (i.e., 58.1 Bq/kg) for 0–20 cm conversion coefficients and the results were shown in Fig. 4. In general, the equivalent doses were found to be higher for the adult female phantom, mainly due to the smaller body size when compared to the adult male phantom. Interestingly, the equivalent doses in the ORNL phantom were found to be generally higher when compared to those from ICRP voxel phantom; these differences would be due to the shape of the modelled organs as ORNL

Table 3
Differences between conversion coefficients (in %) obtained with ICRP and ORNL phantoms
AM male phantom, and AF female phantom.

Statistical differences between both phantoms						
Organ	Depth (cm) → / Phantom	0–5	5–10	10–15	15–20	0–20
RBM	AM	−18.2	−23.1	−30.0	−50.0	−17.4
	AF	−25.0	−28.6	−36.4	−20.0	−27.8
Colon	AM	2.5	9.7	8.3	20.0	6.2
	AF	−1.2	3.2	0.0	0.0	0.0
Lung	AM	−7.8	−12.0	−13.0	−25.0	−6.7
	AF	0.0	0.0	0.0	0.0	0.8
Stomach	AM	−10.3	−7.4	−9.1	0.0	−12.2
	AF	2.6	3.3	0.0	0.0	4.78
Breast	AM	–	–	–	–	–
	AF	−8.1	−11.4	−13.3	−16.7	−10.8
Remainder tissues	AM	8.4	10.7	16.7	20.0	9.6
	AF	7.8	10.0	8.3	20.0	8.1
Gonads	AM	23.4	22.2	22.2	25.0	16.1
	AF	10.8	11.8	7.7	16.7	5.0
Bladder	AM	−4.9	−3.3	0.0	0.0	−6.4
	AF	5.1	5.6	−7.7	0.0	−1.4
Esophagus	AM	−3.8	0.0	0.0	33.3	−6.0
	AF	6.2	8.0	10.0	0.0	4.0
Liver	AM	−4.5	0.0	0.0	0.0	−1.8
	AF	0.0	0.0	0.0	0.0	−0.8
Thyroid	AM	64.9	63.6	62.5	75.0	60.7
	AF	35.9	36.0	36.4	25.0	37.7
Endosteum	AM	−3.2	−8.8	−7.1	0.0	−4.0
	AF	−1.0	−8.6	−14.3	−16.7	−3.3
Brain	AM	–	–	–	–	–
	AF	–	–	–	–	–
Salivary glands	AM	–	–	–	–	–
	AF	–	–	–	–	–
Skin	AM	7.3	6.7	10.5	12.5	6.7
	AF	−22.0	−19.6	−21.0	−25.0	−20.9

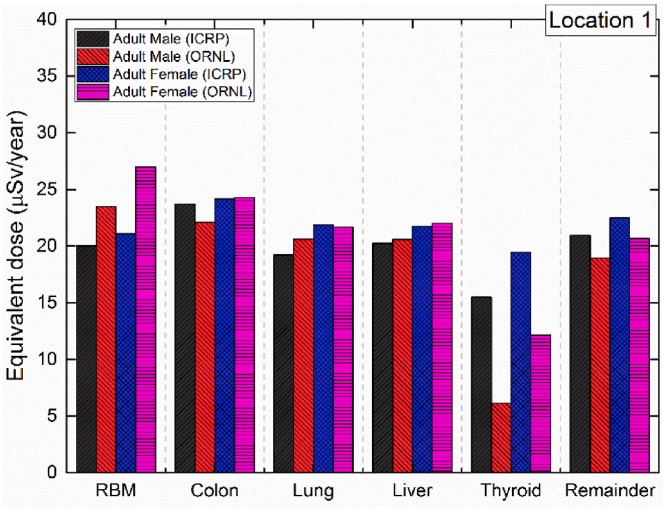

Fig. 4. Equivalent doses for adult male and female ICRP and ORNL phantoms at location 1 for ^{137}Cs contaminated soil at 0–20 cm.

phantoms were built using analytical equations and therefore resembled the organs more roughly. On the other hand, the ICRP voxel phantoms had a more detailed organ structure when compared to those from ORNL phantoms.

It needs to be noted that the equivalent doses can be changed based on the ^{137}Cs activity concentrations. For example, the highest ^{137}Cs activity was measured at location 6, and therefore the equivalent doses in different organs would be significantly higher when compared to other locations. The users can input their ^{137}Cs activity concentrations into the developed program (see Figs. 2 and 3) to obtain specific equivalent doses in different organs for different phantom types.

The effective dose was calculated as the gender average of equivalent doses obtained for all organs and their respective tissue weighting factors. The effective doses calculated for ^{137}Cs activity concentrations at locations 1, 6, and 10 obtained in 2018 and 2001 (see Table 4) were shown in Fig. 5(a) and (b), respectively. The effective doses of the corresponding three sites shown in Fig. 5 were found to be generally lower for samples taken in 2018, except for the samples collected at locations 6 and 11.

In addition, the effective doses for all 11 different locations using ICRP voxel phantom data (ICRP110) for 2018 and 2001 year were found to be 16.66 and 22.63 μSv/y, respectively, which showed a reduction of 26.4% in the mean effective dose from 2001 to 2018. Corresponding values for ORNL phantoms are 15.41 i 20.9 μSv/y for 2018 i 2001, respectively. The reduction of effective doses could not be explained by radioactive decay of ^{137}Cs only. Other processes of ^{137}Cs as translocation and diffusion also influenced on its concentration in soil and conseqently on the total effective dose.

It should be noted that ICRP110 voxel model produced larger doses (in both years) than ORNL phantom-difference is about 8%.

If the outdoor occupancy factor of 0.20 was used (UNSCEAR, 2016), the effective doses in the present work for all 11 locations were estimated to be 3.3 and 3.1 μSv/y for ICRP and ORNL phantoms, respectively. The mean effective dose of 3.3 μSv/y is smaller in comparison to the value 4.5 μSv/y obtained at the same locations in the previous work (Krstić and Nikezić, 2006).

It is remarked that some authors recommended corrections of the occupancy factor to 0.3 in rural and 0.22 in urban areas (Arogunjo, 2004).

As mentioned above, radioactive decay of ^{137}Cs is one of the possible reasons for reducing the doses. This suggests that additional research is necessary, where soil depths, even greater than 20 cm, should be considered. Measurements of the depth distribution of ^{137}Cs in the soil showed that ^{137}Cs, due to the Chernobyl accident, penetrated to a depth of 25 cm (UNSCEAR, 2008). In the present work, it was shown that the soil remains an external source of irradiation for a long time, although the obtained value of 3.3 μSv/y was small in comparison to the effective dose from natural terrestrial sources in the soil, of which the average value was about 0.5 mSv/y (with the typical range of 0.3–0.6 mSv/y) (UNSCEAR, 2000).

There are other research works that have calculated external doses from ^{137}Cs (and ^{134}Cs) in soil. However, direct comparison of the present methodology and those in other research works is not possible. In the paper by Park et al. (2018), the dose was calculated also by MCNP, but the methodology was different from ours. Firstly, they calculated the photon flux on the surface of cylinder with humanoid phantoms. The radius of the cylinder was 100 cm and its height was 200 cm. As a second step, the radiation fluence information recorded in the cylinder was used

Table 4
Average ^{137}Cs activity concentrations measured at different locations.

Measurement location	^{137}Cs activity concentration (Bq/kg), present study, sampling 2018	^{137}Cs activity concentration (Bq/kg), previous study, sampling 2001
1	58.1	64.7
2	22.9	99.3
3	52.6	67.8
4	59.4	44.3
5	25.2	82.5
6	103.5	20.7
7	29.7	59.9
8	53.4	124.1
9	11.3	35.6
10	3.0	31.7
11	56.0	14.9

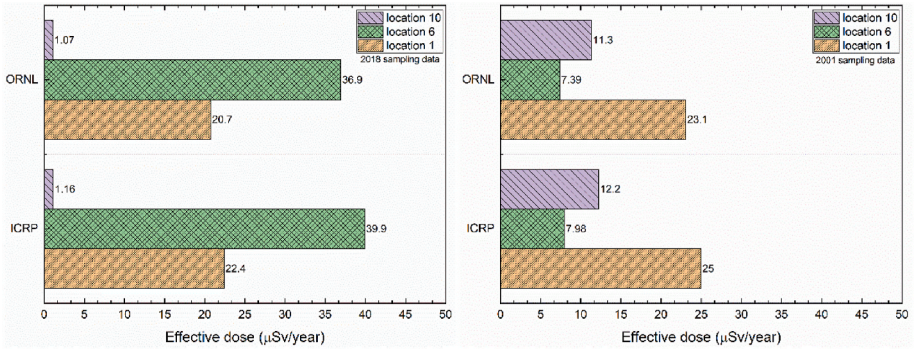

Fig. 5. Effective doses for ICRP and ORNL phantoms from ^{137}Cs activity concentrations in the soil at locations 1, 6 and 10 using sampling data in (a) 2018 and (b) 2001.

to calculate the organ dose with SSW card in MCNPX. There were other differences in comparison to our work: they used a radius of the soil cylinder of 2.5 m, while we used 3 m; their conversion coefficients were given in (mSv/h per kBq/m^2) while we used (fSvs^{-1})/(Bq•kg^{-1}); their results were given up to the depth of 10 cm, while we used 20 cm; they assumed Cs profile to calculate the "radiation dose", while we used data obtained from real on-site measurements. As the most important difference only male phantom was considered in their work. In paper by Silveira et al. (2018), different phantoms (FASH3 and MASH3) were used. The soil was represented by a cylinder with a depth of 2 cm only and 5 m of radius, and ^{137}Cs was uniformly distributed. Furthermore, their soil composition and density were different from ours. Their conversion factors were given as equivalent dose to air Kerma, and effective dose to air Kerma. Their results and our present results are not comparable.

4. Summary and conclusions

In the present work, the vertical profiles of ^{137}Cs in the soil at 11 locations around the city of Kragujevac in central Serbia were analyzed. Two sampling campaigns in 2001 and 2018 were carried out for measurement of ^{137}Cs activity concentrations at different soil depths. In general, a reducing trend of ^{137}Cs activity in soil was observed. However, there is a significant deviation from the expected decline of about 32.5% based on the half-life of ^{137}Cs radionuclide. The obtained data confirms that there are other processes of removal and transfer of ^{137}Cs in the soil that contribute to its reduction and disturb its vertical profile distribution. Although the behavior of ^{137}Cs in soil has been studied for more than 60 years, these results indicate that additional efforts must be made to fully understand the processes of its translocation and diffusion in soil.

In addition to measuring ^{137}Cs concentrations in the soil, the obtained results were used to calculate the effective doses. Two independent models of the human body, the ORNL phantom and the ICRP voxel phantom, were used and difference was found between results produced by them. These differences could be explained by the different geometrical construction of these phantoms and levels of details that were considered in ICRP and ORNL human phantoms. Furthermore, the absorbed doses in female organs were found to be higher than those in male organs; this was due to the smaller height, making it closer to the source that led to higher dose values.

It has also found that ICPR (110) voxel model produce larger doses than ORNL for about 8%. This finding needs further investigation to determine whether a single organ (or group of organs) contributes to this difference or the difference is evenly distributed across all organs considered in both phantoms. Lastly, two open-source computer programs were developed for determination of conversion coefficients in different organs based on the calculated data for four different phantoms presented in this work. The programs are executable on PC and android phones to calculate and report the results of equivalent and effective doses upon user-defined ^{137}Cs activities. The developed program would be a useful tool for future researches in this field from all over the world to determine dosimetric quantities from ^{137}Cs contaminated soil.

Declaration of competing interest

The authors declare that they have no known competing financial interests or personal relationships that could have appeared to influence the work reported in this paper.

Data availability

Data will be made available on request.

Acknowledgments

This work was supported by the Serbian Ministry of Education, Science and Technological Development (Agreement No. 451-03-9/2021-14/200122). The present work was also supported by the Special Grant for the Development of Virtual Teaching and Learning (VTL) no. 6430120 from the University Grants Committee of Hong Kong and by the JSPS KAKENHI grant number 21F21103 and JSPS grant number JPJSBP120218804.

References

Arogunjo, A.M., 2004. A re-evaluation of the occupancy factors for effective dose estimate in tropical environment. Radiat. Protect. Dosim. 112 (2), 259–265. https://doi.org/10.1093/rpd/nch389.

Cristy, M., Eckerman, K.F., 1987. Specific Absorbed Fractions of Energy at Various Ages from Internal Photon Sources. I Methods. Oak Ridge National Laboratory, Oak Ridge, Tennessee, 37831.

Eakins, J., Huet, C., Brkić, H., Capello, K., Desorgher, L., Epstein, L., Hunt, J.G., Kim, H. S., Krstic, D., Lee, Y.-K., Manohari, M., Nikezic, D., Shukrun, R.H., Souza-Santos, D., Tymińska, K., 2021. Monte Carlo calculation of organ and effective dose rates from ground contaminated by Am-241: results of an international intercomparison exercise. Radiat. Meas. 148, 106649 https://doi.org/10.1016/j.radmeas.2021.106649.

Gómez-Ros, J.M., Moraleda, M., Arce, P., Bui, D.-K., Dang, T.-M.-L., Desorgher, L., Kim, H.S., Krstic, D., Kuć, M., Le, N.-T., Lee, Y.-K., Nguyen, N.-Q., Nikezic, D., Tymińska, K., Vrba, T., 2021. Monte Carlo calculation of the organ equivalent dose and effective dose due to immersion in a 16N beta source in air using the ICRP reference phantoms. Radiat. Meas. 145, 106612 https://doi.org/10.1016/j.radmeas.2021.106612.

Goorley, T., 2007. MCNP Medical Physics Geometry Database. Los Alamos National Laboratory. https://mcnp.lanl.gov/pdf_files/la-ur-07-6618.pdf.

Han, E.Y., Bolch, W.E., Eckerman, K.F., 2006. Revisions to the ORNL series of adult and pediatric computational phantoms for use with the MIRD schema. Health Phys. 90 (4), 337–356. https://doi.org/10.1097/01.HP.0000192318.13190.c4.

Huet, C., Eakins, J., Zankl, M., Gómez-Ros, J.M., Jansen, J., Moraleda, M., Struelens, L., Akar, D.K., Borbinha, J., Brkić, H., Bui, D.K., Capello, K., Linh Dang, T.M., Desorgher, L., Di Maria, S., Epstein, L., Faj, D., Fantinova, K., Ferrari, P., Gossio, S., Hunt, J., Jovanovic, Z., Kim, H.S., Krstic, D., Le, N.T., Lee, Y.K., Murugan, M., Nadar, M.Y., Nguyen, N.Q., Nikezic, D., Patni, H.K., Souza Santos, D., Tremblay, M., Trivino, S., Tymińska, K., 2022. Monte Carlo calculation of organ and effective doses

due to photon and neutron point sources and typical X-ray examinations: results of an international intercomparison exercise. Radiat. Meas. 150, 106695 https://doi.org/10.1016/j.radmeas.2021.106695.
IAEA, 2004. Soil Sampling for Environmental Contaminants. IAEA-TECDOC-1415 92-0-111504-0. https://www.iaea.org/search/google/Publication%202004.
ICRP, 2007. Recommendations of the international commission on radiological protection. ICRP publication 103. Ann. ICRP 37 (2–4).
ICRP, 2009. Adult reference computational phantoms. ICRP publication 110 ann. ICRP 39 (2).
ICRP, 2010. Conversion coefficients for radiological protection quantities for external radiation exposures. ICRP Publication 116. Ann. ICRP 40 (2–5), 1–257.
Koo, Y.-H., Yang, Y.-S., Song, K.-W., 2014. Radioactivity release from the Fukushima accident and its consequences: a review. Prog. Nucl. Energy 74, 61–70. https://doi.org/10.1016/j.pnucene.2014.02.013.
Krstić, D., Nikezić, D., 2006. External doses to humans from 137Cs in soil. Health Phys. 91 (3), 249–257. https://doi.org/10.1097/01.hp.0000214136.56619.2d.
Krstic, D., Nikezic, D., 2007. Input files with ORNL—mathematical phantoms of the human body for MCNP-4B. Comput. Phys. Commun. 176, 33–37. https://doi.org/10.1016/j.cpc.2006.06.016.
Krstić, D., Nikezić, D., Stevanović, N., Jelić, M., 2004. Vertical profile of 137Cs in soil. Appl. Radiat. Isot. 61, 1487–1492. https://doi.org/10.1016/j.apradiso.2004.03.118.
Krstic, D., Markovic, V.M., Jovanovic, Z., Milenkovic, B., Nikezic, D., Atanackovic, J., 2014. Monte Carlo calculations of lung dose in ORNL phantom for boron neutron capture therapy. Radiat. Protect. Dosim. 161 (1–4), 269–273. https://doi.org/10.1093/rpd/nct365.
Lamart, S., Bouville, A., Simon, S.L., Eckerman, K.F., Melo, D., Lee, C., 2011. Comparison of internal dosimetry factors for three classes of adult computational phantoms with emphasis on I-131 in the thyroid. Phys. Med. Biol. 56, 7317. https://doi.org/10.1088/0031-9155/56/22/020.
Miri, H.H., Rafat, M.L., Karimi, S.K., 2012. Different effective dose conversion coefficients for monoenergetic neutron fluence from 10-9 MeV to 20 MeV – a methodological comparative study. Radioprotection 47 (2), 271–284. https://doi.org/10.1051/radiopro/2012009.
Park, I., Lee, J., Do, T.G., Kim, M.J., Go, A.R., Kim, K.P., 2018. Calculation of dose conversion coefficients for radioactive cesium in contaminated soil by depth and density. J. Radioanal. Nucl. Chem. 316, 1213–1219. https://doi.org/10.1007/s10967-018-5831-3.
Silveira, L.M., Pereira, M.A.M., Neves, L.P., Perini, A.P., Belinato, W., Caldas, L.V.E., Santos, W.S., 2018. Exposure to 137Cs deposited in soil – a Monte Carlo study. J. Phys. Conf. Ser. 975, 012050 https://doi.org/10.1088/1742-6596/975/1/012050.
Steinhauser, G., Brandl, A., Thomas, E., Johnson, E.T., 2014. Comparison of the Chernobyl and Fukushima nuclear accidents: a review of the environmental impacts. Sci. Total Environ. 470–471, 800–817. https://doi.org/10.1016/j.scitotenv.2013.10.029.
UNSCEAR, 2000. Sources and Effects of Ionizing Radiation. Report to the General Assembly, with Scientific Annexes. United Nations, New York.
UNSCEAR, 2008. Sources and effects of Ionizing Radiation. Report to the General Assembly, vol. II. United Nations, New York.
UNSCEAR, 2016. Sources, effects and Risks of Ionizing Radiation. Report to the General Assembly, with Scientific Annexes, vol. 2017. United Nations, New York.
Wai, K.-M., Krstic, D., Nikezic, D., Lin, T.-H., Yu, P.K.N., 2020. External Cesium-137 doses to humans from soil influenced by the Fukushima and Chernobyl nuclear power plants accidents: a comparative study. Sci. Rep. 10, 7902. https://doi.org/10.1038/s41598-020-64812-9.
Werner, J.C., et al., 2017. MCNP User's Manual, Code Version 6.2. Los Alamos National Security, LLC. Report LA-UR-17-29981.
X-5 Monte Carlo Team, 2003. MCNP-A General Monte Carlo N-Particle Transport Code, Version 5 Vol. I: Overview and Theory. Los Alamos National Laboratory; LA- UR- 03-1987, Los Alamos, NM.
Xu, X.G., 2014. An exponential growth of computational phantom research in radiation protection, imaging, and radiotherapy: a review of the fifty-year history. Phys. Med. Biol. 59, R233. https://doi.org/10.1088/0031-9155/59/18/R233.
Zankl, M., Eakins, J., Gómez Ros, J.-M., Huet, C., 2021. The ICRP recommended methods of red bone marrow dosimetry. Radiat. Meas. 146, 106611 https://doi.org/10.1016/j.radmeas.2021.106611.
Zivkovic, M., Zlatic, N., Zeremski, T., Stankovic, M., Manic, V., Krstic, D., Nikezic, D., 2022. Ecological studies of the naturally occurring radionuclides, 137Cs and heavy metals in soil, plants and milk in surrounding of Kragujevac city, Serbia. J. Radioanal. Nucl. Chem. 331 (3), 1285–1298. https://doi.org/10.1007/s10967-022-08202-7.